1.9 OBSERVATIONS OF PRECIPITABLE WATER VAPOR IN THE PLANETARY BOUNDARY LAYER VIA MICROWAVE INTERFEROMETRY

X. M. Shao[1]*, R. Carlos, M. Kirkland
Space and Atmosphere Science Group, Los Alamos National Laboratory, New Mexico

1. ABSTRACT

A 9-antenna, 400 meter microwave interferometer was utilized in SALSA-MEX campaign in the San Pedro River Riparian National Conservation area in July and August, 1997, to measure the turbulence in the Convective Boundary Layer. Water vapor has an appreciable index of refraction at radio frequencies around 10 GHz, and acts as a passive tracer of the magnitude and motion of turbulence. The relative phase changes of a signal from a satellite were tracked by an array of 9 antennas, and the phase differences between antennas were then used to derive the turbulence properties of the boundary layer. Preliminary analysis shows clearly different characteristics for the convection activity of the boundary layer between day and night. From the structure function analysis we can see that the turbulence structure starts to decorrelate at scale sizes of 200 meters for a temporal passband around 100 seconds. Derivation of average wind fields from the interferometric measurements is currently being pursued.

2. INTRODUCTION AND CONCEPT

It is possible to measure the turbulence in the Convective Boundary Layer (CBL) by observing a microwave transmitter above the layer (such as a satellite) with an array of receivers on the ground. A microwave interferometer is relatively inexpensive to construct and can be operated continuously and remotely since it has no moving parts and no need for operator adjustment.

An interferometer works by measuring the phase difference of one signal as received at pairs of spatially separated antennas. Each antenna does not serve as a 'local' sensor but as a reference for the antenna at the opposite end of the baseline. The baseline phase difference is then a measure of the horizontal gradient of the electrical path length from the satellite to the antennas. Each cm of precipitable water vapor causes about 6.45 (± 0.1) cm of extra electrical path length. At microwave frequencies, water vapor integrated along the line-of-sight is the principle cause of phase delay, and so our measurement of phases at horizontally spaced antennas leads directly to a structure function; e.g, Tatarski (1961) investigation of the variance of the column-integrated water vapor content. Structure functions, or more precisely phase structure functions, have been commonly used by radio-astronomers for characterizing water vapor irregularities; e.g., Armstrong and Sramek, (1982).

Herein we present observations that were conducted as part of the Semi-Arid Land Surface Atmospheric Interactions (SALSA) campaign near the San Pedro river, east of Sierra Vista, in southern Arizona during July and August, 1997.

3. THE MICROWAVE INTERFEROMETER

A geostationary television satellite, GSTAR-4, located at 105 degrees west longitude, has a continuous beacon at about 11.7269 GHz. It was well positioned for our observations from southern Arizona at an azimuth of 170 degrees and an altitude of 53 degrees.

The interferometer consisted of an X-pattern array of nine 1.5 m antennas, the arms orthogonal to each other, as shown in Figure 1. The spacing between antennas was 100 meters, and the total size of the array was 400 m by 400 m.

At the focus of each antenna, a feed horn fed directly into a preamplifier/down-converter with 55 db gain and output at 406.9 MHz. The local oscillator for the down-converter was derived by up-converting at the antenna a common reference signal distributed from the central facility to all antennas.

[1]* *Corresponding author address:* X. M. Shao, NIS-1, MS D466, Los Alamos National Laboratory, Los Alamos, NM 87545. E-mail: xshao@lanl.gov

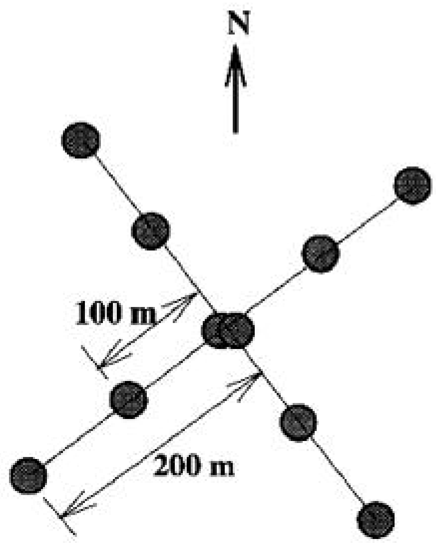

Figure1. Antenna array of the water vapor microwave interferometer.

The reference signal (at 157.222222 MHz) and the data signal (at 406.9 MHz) are multiplexed on the same cable and sorted by filters at both ends. It is critical that the electrical length of the cables remain constant over the time period of interest. Since the measurements that are being made are the phases of the signal received at the antennas and if the phase-length of the cable changes, the apparent phase at the central facility will change too.

To shield the cable from sun, clouds, wind, and rain, it was buried 20 cm deep, and all exposed portions at the antennas were insulated. The exposed sections at the central facility were insulated together, so that most temperature fluctuation would be common to all signals.

At the central facility, the incoming signals were first separated from the outgoing reference signal, and then mixed down to the High Frequency band at 26.9 MHz. The local oscillator was derived from the signal of the central antenna, and so common mode fluctuations in the frequency or phase were subtracted out of the signals at all the other antennas. Some examples of common mode fluctuations are changes in the satellite's frequency, local noise insofar as it is uniform through the array, and instabilities in the reference frequency synthesizer.

The HF signals were fed into radios that amplify, filter with a 100 Hz bandpass, and down-convert to a 20 Hz output, which was then digitized at 80 samples/sec/channel and recorded on computer disk. The data were archived daily onto CD-ROMs.

In addition to the 9 antennas of the array, a 10th antenna was positioned next to the central antenna as a witness antenna. The central antenna itself had a 5 meter cable run back to the facility; the 10th antenna had a 200 meter run out and back, so that the effects of temperature on the cable could be quantified by comparing the signals from two antennas which should be identical.

4. **Observations and Preliminary Results**

In this paper, we present preliminary observation results obtained on August 11, 1997. As described above, our interferometer measures phase differences between pairs of antennas, which are caused by changing water vapor content integrated along the lines of sight.

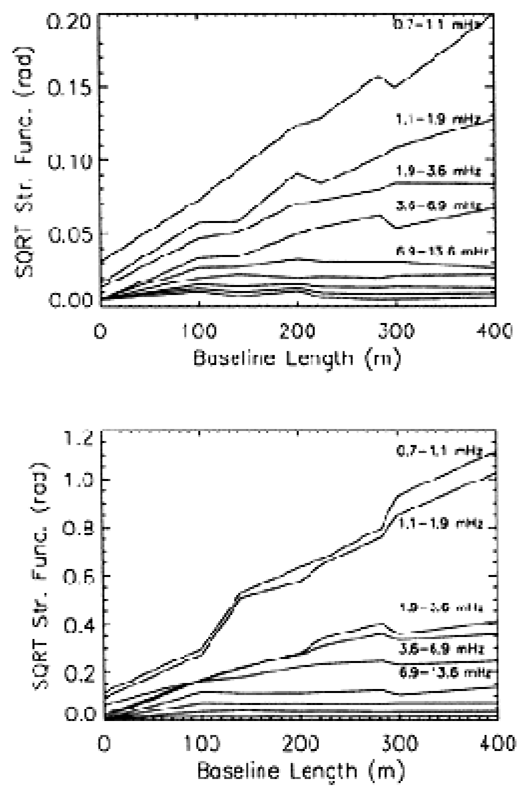

Structure

Figure 2. Square-root of the phase structure functions vs baseline length for 9 successive frequency successive octaves. (a) at 1:00 and (b) at 14:00 on August 11, 1997

function has been commonly used for describing the spatial statistics of the turbulent boundary layer; e.g., Tatarski, (1961). For a random function

$f(\boldsymbol{r})$, the structure function is defined as:

$$D_f(\boldsymbol{r}, \boldsymbol{R}) = \langle (f(\boldsymbol{r} + \boldsymbol{R}) - f(\boldsymbol{r}))^2 \rangle$$

where ***r*** is a vector in space, ***R*** is a displacement. The angle brackets denote the ensemble average. In our case, we have measured the phase of the microwave signal and so we have a phase structure function.

Our interferometer consists of 9 spatially separated antennas in a 400 by 400 meters area. This gives $9 \times 8/2 = 36$ unique baselines, ranging from 0 to 400 meters. If we assume that the atmosphere over the interferometer is isotropic, all of the equal-length baselines can be treated identically, regardless their orientations and locations. This assumption is roughly valid, at least in the region above the frictional layer (tens of meters above ground) as found by other investigators; e.g., Caughey and Palmer (1979) and Kaimal et al. (1976). The structure function therefore can be reduced from a vector equation to a scalar equation. The multiple equal-length baselines (for instance, eight 100 m baselines) would then statistically improve the turbulence measurements. Rather than estimate the structure function over the entire temporal frequency band, we will investigate it at consecutive passbands, following the technique introduced by Jacobson and Sramek (1997), in order to bring out the effects of different scale sizes. Each temporal frequency band would correspond roughly to a certain spatial scale of the boundary layer turbulence if a frozen flow assumption is reasonably valid.

Figure 2a and 2b show the square-root of the phase structure functions versus baseline length for 9 successive frequency octaves, at local time 1:00 and 14:00 on August 11, 1997, respectively. The structure function is computed over a two hour time window centered at the chosen times. The frequency passbands, starting from 0.7-1.1 mHz (the top curve, 1440-900 seconds in temporal scale), double consecutively as labeled in the figure. The square-root of the phase structure function has units of radians/$\sqrt{Hz}$ and is linearly related to the column water vapor content. The phase value at each baseline length is an average of all the available equal-length baseline measurements. The 0 meter baseline measurement is solely from the witness antenna, which was co-located with the central antenna, thus providing a measure of the system noise level.

Figure 2a shows the observations at 1:00 local time, the time at which the boundary layer activity is expected to be relatively stable. As shown in the figure, the spectral power decrease as the frequency increases. This agrees in general with the theory for a stationary isotropic turbulence field. One also notices that as the frequency increases, the structure function starts to 'saturate'. For instance, at 6.9-13.6 mHz (144-73 seconds), the structure function reaches maximum at about 200 meters. Moreover, we note that in general the saturation length decreases as the frequency further increases, as found by Jacobson and Sramek (1997) from similar measurements taken with the National Radio Astronomy Observatory's Very Large Array (VLA). The saturation of the structure function indicates that the turbulent water vapor properties begin to decorrelate from one location to the other, which is to say, the eddy scale becomes comparable or smaller than the observing distance and the isotropy and homogeneity no longer apply. In the case of Figure 2a, the eddy scale at 6.9-13.6 mHz passband does not exceed significantly the 200 meter baseline length.

Observations at 14:00 (Figure 2b) show clear differences compared to those observations at 1:00. This is the time of a day that one would expect the boundary layer convection to become most vigorous. These results clearly demonstrate this expectation. The spectral power at this early afternoon time is several times greater than that of the midnight. The greater spectral power indicates the boundary layer is more unstable. Alternatively, the water vapor content over the interferometer array is less spatially uniform. With a more turbulent field one would expect the saturation length of the structure function at a given temporal frequency to become shorter. In fact, Figure 2b shows that the saturation length is about 300 meters in the 6.9-13.6 mHz passband, greater or at least no less than it was at 1:00. A plausible explanation for this is the horizontal wind speed. A higher wind field would carry the turbulence structure more quickly over the spatially separated antennas, therefore effectively increasing the saturation length.

Figure 3 illustrates the diurnal variation of the square-root of the phase structure function in 6

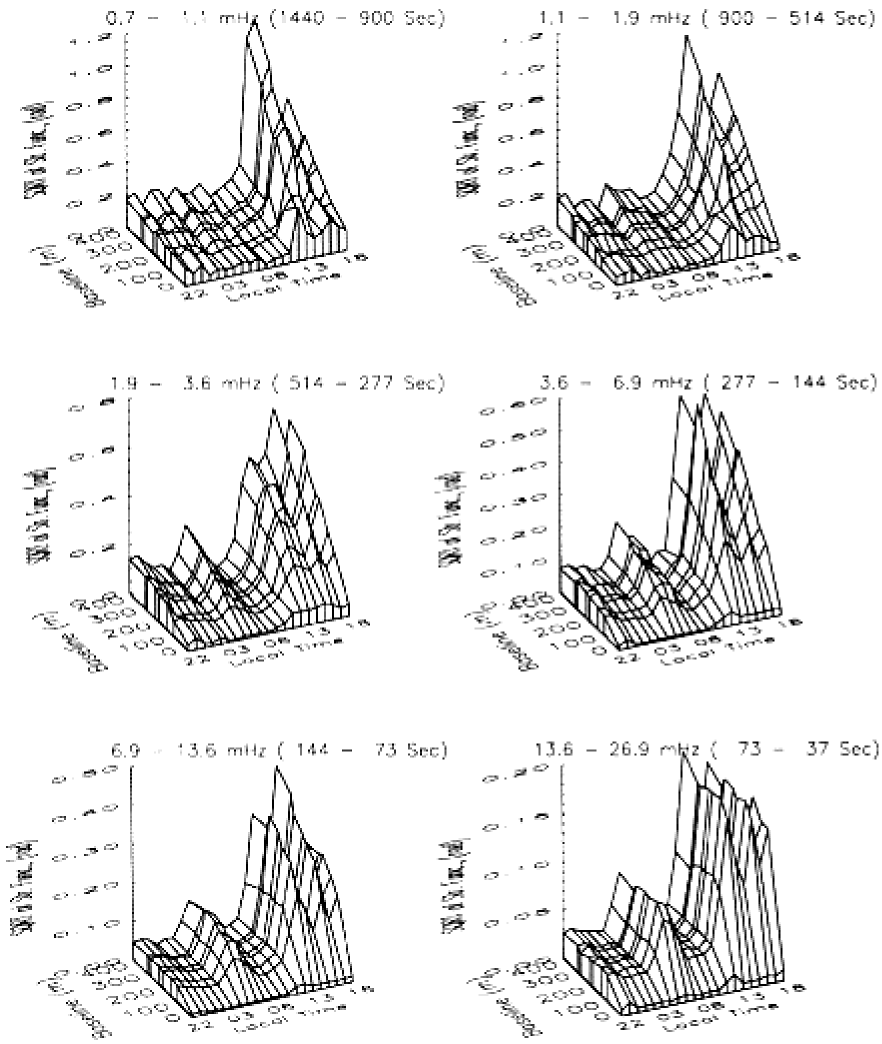

Figure 3. Figure 3. Diurnal variations of CBL turbulence, at successive temporal frequency passbands.

successive frequency passbands. As an overview one can see clearly, at least from the low frequency passbands (or long temporal scale), that the boundary layer convection was relatively stable at night and in the early morning and became most active in the late afternoon. Closer examinations reveal several interesting points. First, there was a relatively active period around 5:00 as shown in the 3rd to the 6th passbands (periods less than 514 seconds). This activity decayed gradually toward 8:00, about one and a half hour after sunrise. Secondly, after 8:00, convection at all scales became increasingly active. The lower frequency components (first two passbands) peaked at about 14:00, while the higher frequencies peaked at 13:00, an hour earlier. And thirdly, the convection intensity appeared to oscillate in the afternoon hours at a repetition rate of 2-3 hours at high frequency passbands; it was less obvious in the lower frequencies.

5. SUMMARY

We have developed a microwave interferometer dedicated to CBL water vapor measurement. This measurement technique is based on the fact of that precipitable water vapor dominates the electrical path length changes at microwave frequencies. Precipitable water vapor acts as a passive tracer in the convective atmosphere and it mostly resides within the CBL. An interferometer provides an additional tool for

CBL studies. They are relatively cheap and can be operated continuously, automatically, and remotely.

The interferometer essentially measures the fluctuations of the integrated-column water vapor. Preliminary results derived from the interferometer observations show clearly the diurnal variations of the CBL turbulence activities (Figure 3). Careful examinations of the results appear to reveal a number of interesting turbulence characteristics, for instance, the pre-morning activity, the later afternoon oscillation, and the structure decorrelation over 200-300 meters for the 100 seconds temporal scale, as described in the last section. The average wind field over the interferometer antenna array can also be derived, and is in the process as we are writing up this paper.

6. **Acknowledgment**

This work was performed under the auspices of the Department of Energy.

7. **References:**

Armstrong, J.W., and R.A. Sramek, 1982: Observations of tropospheric phase scintillations as 5 GHz on vertical paths. *Radio Science,* **17**, 1578-1586.

Caughey, S.J., and S.J. Palmer, 1979: Some aspects of turbulence structure through the depth of the convective boundary layer. *Quart. J. R. Met Soc.,* **105**, 811-827.

Jacobson, A.R., and R. Sramek, 1997: A method for improved microwave-interferometer remote sensing of convective-boundary-layer trubulence, using water vapor as a passive tracer. *Radio Science,* in print.

Kaimal, JC., J.C. Wyngaard, D.A. Haugen, O.R. Cote, Y. Izumi, S.J. Caughey, and C.J. Readings, 1976: Turbulence structure in the convective boundary layer, *J. Atmos. Sci.,* **33**, 2152-2169.

Tatarski, V.I., 1961: Wave propagation in a turbulent medium. Dover, New York.